MRI images series segmentation using the geodesic deformable model

Israa A. Alwan [1], Faaza A. Almarsoomi [2]

[1,2] Department of Computer Science, Faculty of Education for Pure Sciences ibn Al-Haitham, University of Baghdad

ABSTRACT

Image segmentation is regarded as the most crucial medical imaging process because it extracts the region of interest and thus helps upgrade medical diagnosis. The Geodesic deformable model is a curve that deforms within digital images to extract object shapes. The Geodesic deformable model has been used very successfully in the process of single image segmentation but it fails to segment a series of images. In this research, the Geodesic deformable model is developed to overcome its limitation by controlling the speed of the curve deformation.

The developed model is implemented on several series of MRI images that include tumors of varying shape complexity. Experimental results show that the developed model performed very well and successfully segmented the series of MRI images which outperform the baseline model.

Keywords: MRI Image, Open-source framework, Arabic word similarity, Geodesic Deformable

Corresponding Author:

Faaza A. Almarsoomi
Department of Computer Science, Faculty of Education for Pure Sciences Ibn Al-Haitham
University of Baghdad, Iraq
E-mail: faaza.a.a@ihcoedu.uobaghdad.edu.iq

1. Introduction

Generally, segmentation is the process of partitioning an image into regions that have the same properties such as texture, color, contrast, and brightness [1]. As the segmentation process results are robust and have a high degree of accuracy, it is very much helpful for the analysis of different medical images, like magnetic resonance imaging (MRI) images, computerized tomography (CT) images, and Ultrasound images [2]. Concerning medical images analysis, segmentation is the process of separating organs or lesions of interest from other parts of the body [3, 4]. It is considered one of the most challenging tasks because it delivers critical information about the shape and volume of the region of interest and the physician's decision depends on this information [3, 4]. In this research, the Geodesic deformable model is used to segment a lesion, not an organ from a series of MRI images. This lesion is a (brain tumor). Magnetic Resonance Imaging (MRI) is considered because it is the approved imaging modality for fixing brain tumors [5].

A Geodesic deformable model is a curve that deforms within digital images to extract object shapes [6]. There are two types of the Geodesic deformable model. These are the Region-based geodesic deformable model and the Edge-based geodesic deformable model. The Region-based geodesic deformable model is based on either the variance in and out the curve or the squared difference between average intensities in and out the curve along with the total curve length. This type of Geodesic deformable model supports different image features not only edges. In this type, the segmentation of multiple regions is not possible [7].

The Edge-based geodesic deformable model which defines a geometric flow curve evolution depending on the gradients of boundaries in the image that undergoes curve segmentation. The edge-based geodesic deformable model owns fast computation speed and an intrinsic formulation in such a way that it does not depend on the parameterization so, it can be represented as an embedded curve of a higher dimensional function. This

representation gives the geodesic deformable model the good ability to process the singularities and the topological changes [7, 8, 9].

The advantages of the second type meet with the research problem, where the fast computation speed is required because we have a series of brain MRI images. Also, the ability to process the singularities and the topological changes is required because the shapes of brain tumors are often irregular. For these reasons, the second type is considered in this research.

The Geodesic deformable model was introduced by *Caselles et al* [10]. In the beginning, they had some of the fundamental problems, but fortunately, they were solved as we shall explain later. As for the research problem, The Geodesic deformable model uses the following mathematical equation:

$$\frac{\partial P(t)}{\partial t} = F. \vec{N} = \vec{v}$$ ……………. (1)

The basis is to make evolve a curve P under the action of a force F in the direction of its normal $\vec{N}$ at a speed $\vec{v}$. The Geodesic deformable model uses an evolution speed expression which depends on the gradient of the original image. This speed is either constantly positive or constantly negative what makes the evolution of curve in only towards the inside or towards outside but not in the two directions together [11]. In other words, the initial curve must be inside or outside the desired object but cannot be across it. This last point is a major disadvantage if we want to perform segmentation on a series of MRI images. In this research, the limitation of this model is overcome by controlling the speed of the curve evolution. The developed model is applied to several series of synthetic images and several series of brain MRI images (real cases).

2. Method

2.1. Geodesic deformable models

As mentioned before, the Geodesic deformable model was introduced by *Caselles et al* [10]. They proposed the geometric minimization problem:

$$\min_{P \subset \Omega} F(P) = \int_0^{L(P)} f\big(|\nabla I_0(P(s))|\big)ds$$ ……………. (2)

where ds is the Euclidean factor of length, $L(P)$ is the length of the planar closed curve P, Ω is the domain of the image, I_0 is a given image and f is an edge detecting function that disappears at object boundaries such as the one defined in the following Equation:

$$f(I_0) = \frac{1}{1 + \gamma |\nabla(I_0 * G_\sigma)|^2}$$ ……………. (3)

where G_σ is the Gaussian function with standard deviation σ, $I_0 * G_\sigma$ is a smoothed form of the given image I_0 and γ is an arbitrary positive constant.

The calculus of variations gives the Euler-Lagrange equation of Functional F and the gradient descent scheme provides the flow that minimizes F:

$$\partial_t P = (kf - \langle \nabla f, N \rangle)N$$ ……………. (4)

where k is the curvature and N is the normal to the curve. The use of embedding techniques [12] in representation of geodesic deformable model makes it able to solve the problem of curve deformation as well as deal with singularities and topological changes. Equation (4) can be written in the embedding form as follows [13]:

$$\partial_t \varphi = \left(kf + \langle \nabla f, \frac{\nabla \varphi}{|\nabla \varphi|} \rangle\right) |\nabla \varphi|$$ ……………. (5)

where φ is the embedding function which embeds the curve P.

The main problems of this variational segmentation model are first, the unstable evolution of the embedding function, where it requires frequent re-distancing to signed distance function. Second, the slow evolution because of the small-time step [14].

In 2005, Chunming *et al* [15] advised a new variational formulation that forced the embedding function to be close to a signed distance function and therefore eliminated the need for the costly re-distancing procedure. The energy function consists of a Correction term and a Stopping term, respectively. The Correction term $C(\varphi)$ corrects the deviation of the embedding function from a signed distance function, whereas the Stopping term $\psi(\varphi)$ drives the motion of the embedded initial curve to the desired object boundaries.

The resulting evolution of the embedding function is the gradient flow that minimizes the total energy functional. The equation of the energy function is:

$$\varepsilon(\varphi) = \mu\, C(\varphi) + \psi_{f,\lambda,\upsilon} =$$
$$\mu \int_\Omega \frac{1}{2} (|\nabla\varphi| - 1)^2 \, dxdy + \lambda \int_\Omega f\delta(\varphi)|\nabla\varphi| dxdy + \upsilon \int_\Omega fH(-\varphi)dxdy \qquad \text{..............} \textbf{(6)}$$

where μ is a parameter supervising or controlling the effect of correcting the deviation of φ from a signed distance function, and f is the edge detecting function as predefined in Equation (3).

The evolution equation (the gradient flow) is:

$$\frac{\partial\varphi}{\partial t} = -\frac{\partial\varepsilon}{\partial\varphi} \qquad \text{..............} \textbf{(7)}$$

where $\frac{\partial\varepsilon}{\partial\varphi}$ is the Gateaux derivative (first variation) of the energy functional.

The formulation proposed by Chunming *et al* [15] has three main advantages over the formulations of traditional embedding techniques. First, the embedded curve evolution became faster because a considerably larger time step can be used for numerically solving it. Second, the initialization of the embedding function could be as the functions that are computationally more efficient to generate than the signed distance function. Third, the embedded curve evolution can be carried out using a simple finite difference scheme, instead of a complex upwind scheme as in traditional formulations [14].

Despite these valuable improvements, the Geodesic deformable model still has the limitation of the initial curve position. The initial curve must be inside or outside the desired object but cannot be across it. The reason for this is due to the coefficient υ of the stopping term in Equation (6). The value of coefficient υ can be positive or negative, according to the relative position of the initial curve to the desired object. For example, if the initial curve is placed outside the desired object, the coefficient υ should take a positive value, so that the curve can shrink faster towards the boundaries of the object. If the initial curve is placed inside the object, the coefficient υ should take a negative value to speed up the expansion of the curve towards the boundaries of the object.

This condition is a major constraint if we want to perform segmentation on a series of MRI images. The initial curve is placed by the user on the first MRI image only. As for the rest of the MRI images, the initial curve is placed automatically (The final curve of the current MRI image is used as the initial curve for the next MRI image), so the initial curve position may be across the boundaries of the brain tumor, which leads to the wrong segmentation result. The value of υ can neither be negative nor positive. This limitation will be addressed in this research. An example of this limitation is shown in Fig (1).
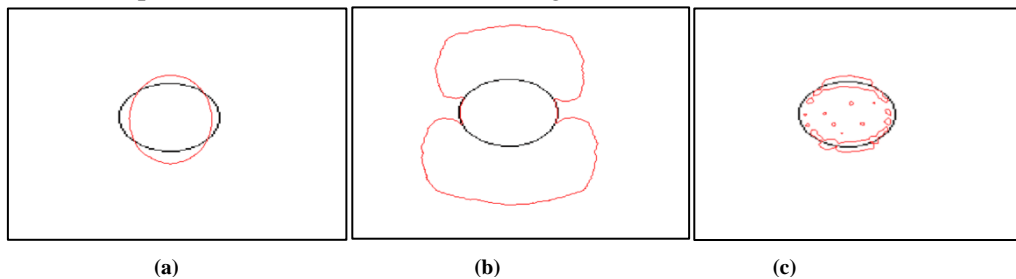

| (a) | (b) | (c) |

Figure 1. Limitation of the initial curve position. (a) the initial curve in red color is across the desired object, (b) The coefficient υ has a negative value, so the curve is expanded outside the object boundaries, leading to wrong segmentation, and (c) The coefficient υ has a positive value, so the curve is shrunk within the object boundaries, leading to wrong segmentation

2.2. The developed segmentation model

In our developed model, the segmentation of the MRI images series is performed by always keeping the curve inside the tumor region. For the first MRI image, the initial curve is placed inside the tumor region by the user, and after the initial curve has evolved in a certain percentage (to be defined by the user according to the tumor shape complexity) the curve is kept so that it is automatically reused as the initial curve for the next MRI image and so on for the rest of the MRI images.

In other words, the final curve of the current MRI image is not used as the initial curve for the next MRI image, but rather the curve is used in an intermediate stage of its evolution so that the curve is still inside the tumor region as clarified in the algorithm below:

Segmentation algorithm of MRI Images Series
Input: Series of MRI images.
Output: Segmented series of MRI images.
Step1: Start
Step2: Input the No. of MRI images in the series (MRINo.).
Step3: Input the value of the Evolution Percentage (EP) (according to the tumor shape complexity across the series).
Step4: For I=1 to MRINo.
Step5: Load the MRI image(I).
Step6: Input the values of the parameters: Sigma(σ), Epsilon(ε), Delt(T), Lambda(λ), Alf(v), and the evolution iterations No. (IterNo.).
Step7: Find the edge detection function (*f*) for the loaded MRI image.
Step8: Find the Mu(μ) value, where Mu=0.2/Delt(T).
Step9: If I=1, take the Initial Curve from the user (the initial curve must be placed inside the tumor region), otherwise Initial Curve = IntermedU.
Step10: By using the Initial Curve, find the Initial embedding function (U).
Step11: Start the evolution of the Initial embedding function (U)
      For N = 1 to IterNo.
Step12: By using mu(μ), find the Correction Term.
Step13: By using Lamda(λ), Epsilon(ε), and Alf(v), find the Stopping Term.
Step14: Update the Initial embedding function (U)
      U = U + Delt(T) * (Correction Term + Stopping Term)
Step15: If the evolution of the embedding function (U) reaches a percentage equal to that specified by the user (EP), then keep the current evolved function.
      If N = round(IterNo. * EP)
          IntermedU = U
Step16: Next N
Step17: Next I
Step18: Stop

3. Experimental results

The developed segmentation model is implemented and tested on several synthetic and MRI images series. These series include objects of varying shape complexity as will be explained in the following sections. The MRI Images series that were used in this experiment are real cases[12].

---

1 Radiopaedia is An open-edit radiology resource, assembled by radiologists and other health professionals from around the world.
  Available at: http:// www. Radiopaedia.org/cases/

2 The Whole Brain Atlas of Medical School, Harvard University. Available at: http:// www.med.harvard.edu/ANNLIB

3.1. Series of the synthetic images

The developed model is applied to two series of synthetic images. The first series includes an object of a regular shape (elliptical object). As we can see in Fig (2), the dimensions of the object are constantly increasing (the object boundaries are continuously diverging from its center) across the images of the series. This means that the current evolving curve can be kept as the initial curve for the next image after a fair percentage of evolution has been achieved. So in this experiment, the suggested value of (EP) was 25%, note Fig (3). The final segmentation result is shown in Fig (4), where our developed model can segment the entire series. The parameters that were used for this series are shown in Table (1).

The second series includes an object of an irregular shape. As we can see in Fig (5), the dimensions of the object are changing randomly (the object boundaries approach its center at times and diverge at other times) across the images of the series. This means that the current evolving curve can be kept after a small percentage of evolution has been achieved. This is to ensure that the initial curve does not touch the object boundaries in the next images. So in this experiment the suggested value of (EP) was 13%, note Fig (6). Final segmentation result is shown in Fig (7), where our developed model can segment the entire series. The parameters that were used for this series are shown in Table (2).
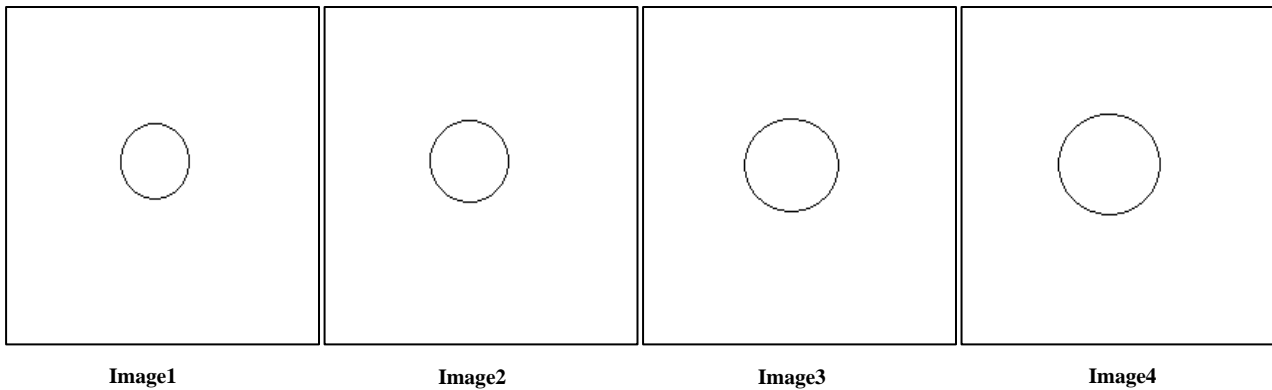

Figure 2. Series of synthetic images includes an object of a regular shape
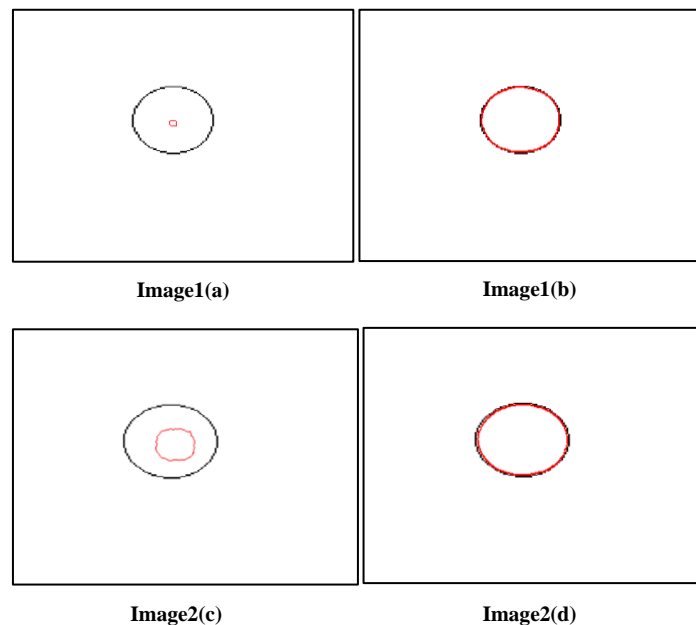

Figur 3. Initialization of first and next image. (Image1(a)) The initial curve in red color is given by the user, (Image1(b)) the final curve, (Image2(c)) After the initial curve of Image1 evolved by 25% , it was kept and automatically reused as the initial curve for the Image2, (Image2(d)) the final curve
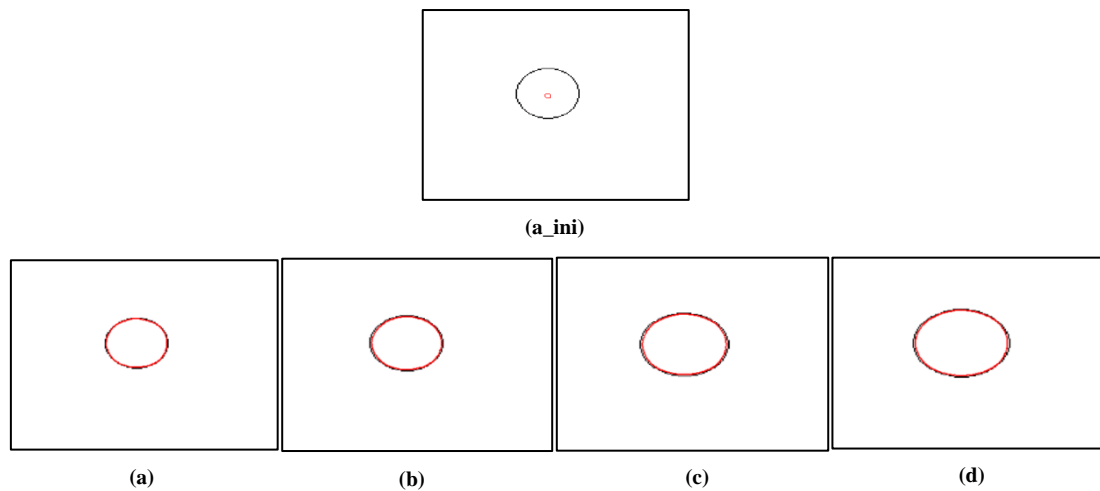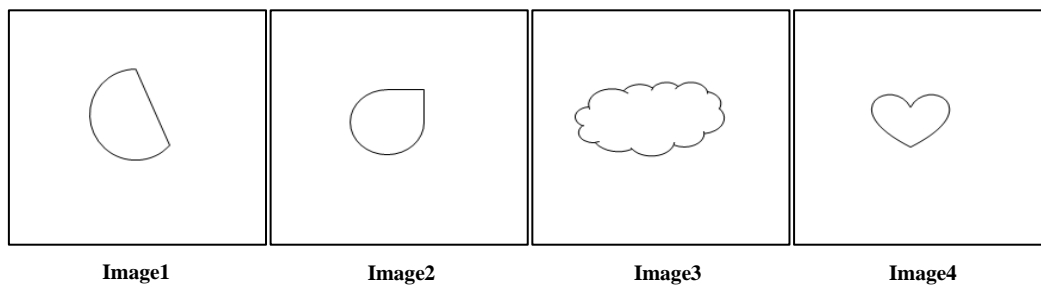
(a_ini)

(a) **(b)** **(c)** **(d)**

Figure 4. Segmentation result of the entire series. (a_ini) Initial curve in red color, (a), (b), (c), and (d) final curves

Table 1. Segmentation process parameters of the first synthetic images series

Image No.	Sigma(σ)	Mu(μ)	Lambda(λ)	Epsilon(ε)	Alf(υ)	Delt(T)	IterNo.
1	1.5	0.06	3	1.5	-6	3	200
2	1.5	0.1	3	1.5	-6	2	155
3	1.5	0.1	3	1.5	-3	2	150
4	1.5	0.1	3	1.5	-3	2	150

Image1 **Image2** **Image3** **Image4**

Figure 5. Series of synthetic images includes an object of an irregular shape

Image1(a) **Image1(b)**
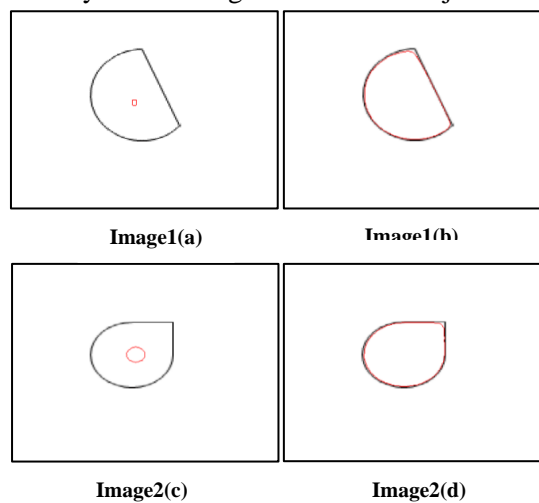

Image2(c) **Image2(d)**

Figure 6. Initialization of first and next image. (Image1(a)) The initial curve in red color is given by the user, (Image1(b)) the final curve, (Image2(c)) After the initial curve of Image1 evolved by 13% , it was kept and automatically reused as the initial curve for the Image2,(Image2(d)) the final curve

(a_ini)

(a)   **(b)**   **(c)**   **(d)**
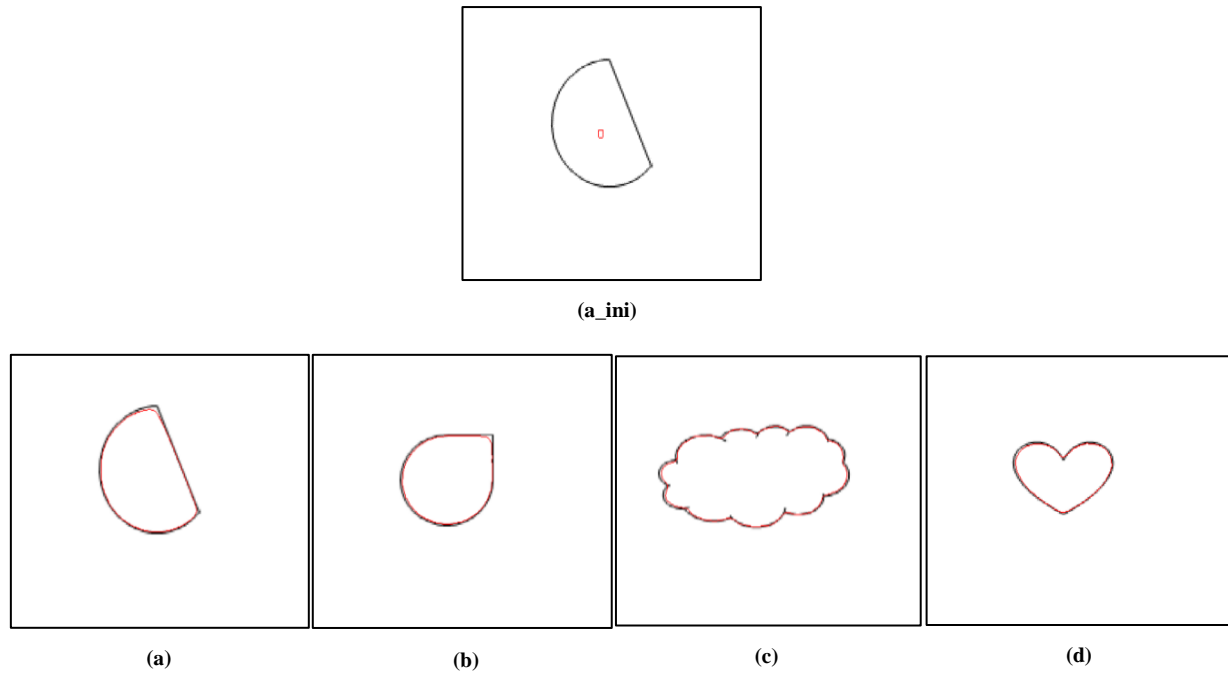
Figure 7. Segmentation result of the entire series. (a_ini) Initial curve in red color, (a), (b), (c), and (d) final curves

Table 2. Segmentation process parameters of the second synthetic images series

Image No.	Sigma(σ)	Mu(μ)	Lambda(λ)	Epsilon(ε)	Alf(v)	Delt(T)	IterNo.
1	1.5	0.06	3	1.5	-6	3	250
2	1.5	0.1	3	1.5	-3	2	300
3	1.5	0.1	3	1.5	-3	2	510
4	1.5	0.1	3	1.5	-3	2	250

3.2. Series of the MRI images

The developed model is applied to three series of MRI images. The first series includes a tumor of a regular shape. The tumor boundaries are continuously diverging from its center across the series of MRI images. As mentioned before, the current evolving curve can be kept after a fair percentage of evolution has been achieved. So, the suggested value of (EP) was 25%. The final segmentation result is shown in Fig (8). The parameters that were used for this series are shown in Table (3).

The second series includes a tumor of a somewhat irregular shape. The tumor boundaries are also continuously diverging from its center across the series of MRI images. So, the suggested value of (EP) was also 25%. The final segmentation result is shown in Fig (9). The parameters that were used for this series are shown in Table (4).

The third series includes a tumor of an irregular shape. The tumor boundaries approach its center at times and diverge at other times across the series of the MRI images. The current evolving curve can be kept after a small percentage of evolution has been achieved. This is to ensure that the initial curve does not touch the tumor boundaries in the next MRI images. So, the suggested value of (EP) was 13%. The final segmentation result is shown in Fig (10). The parameters that were used for this series are shown in Table (5).

(Image1_ini)

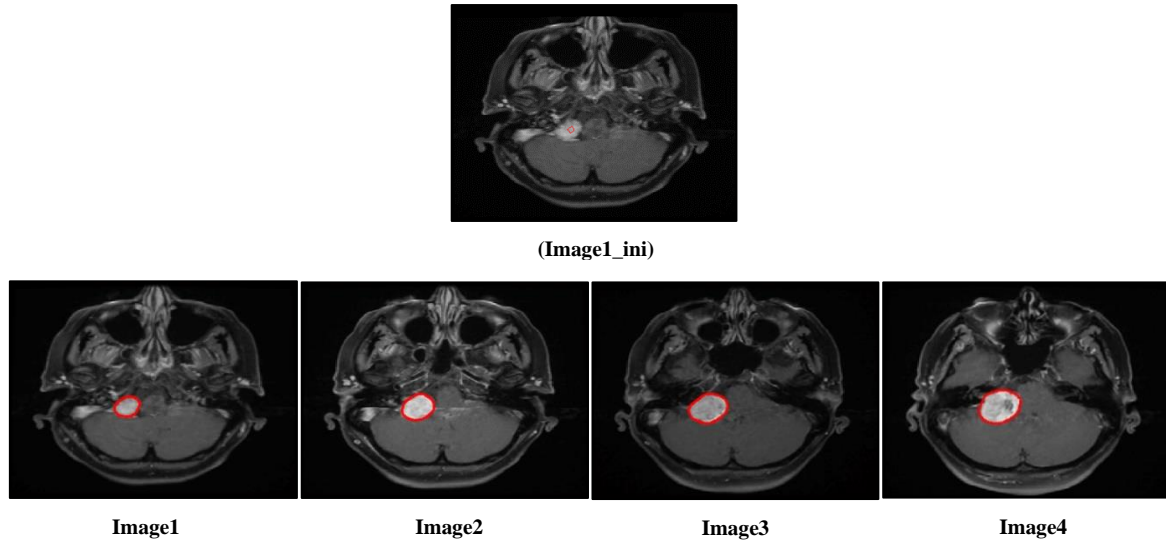| Image1 | Image2 | Image3 | Image4 |

Figure 8. Segmentation result of the first MRI images series. (Image1_ini) Initial curve in red color, (Image1), (Image2), (Image3), and (Image4) final curves

Table 3. Segmentation process parameters of the first MRI images series

Image No.	Sigma(σ)	Mu(μ)	Lambda(λ)	Epsilon(ε)	Alf(υ)	Delt(T)	IterNo.
1	1.5	0.06	3	1.5	-6	3	300
2	1.5	0.1	3	1.5	-6	2	200
3	1.5	0.1	3	1.5	-3	2	250
4	2	0.06	3	1.5	-8	3	210

(Image1_ini)

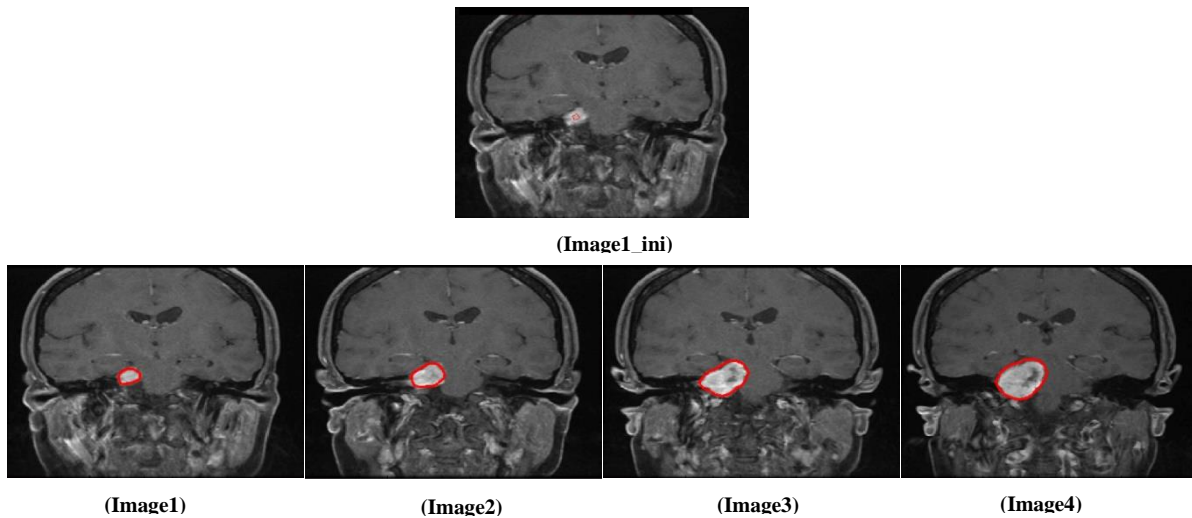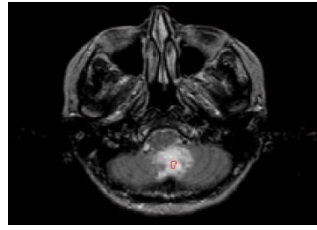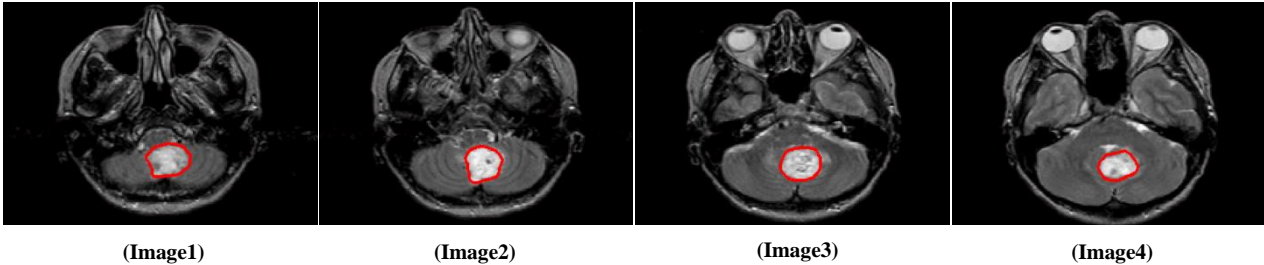| (Image1) | (Image2) | (Image3) | (Image4) |

Figure9. Segmentation result of the second MRI images series. (Image1_ini) Initial curve in red color, (Image1), (Image2), (Image3), and (Image4) final curves

Table 4. Segmentation process parameters of the second MRI images series

Image No.	Sigma(σ)	Mu(μ)	Lambda(λ)	Epsilon(ε)	Alf(υ)	Delt(T)	IterNo.
1	1.5	0.06	3	1.5	-3	3	250
2	1.5	0.1	3	1.5	-6	2	300
3	2	0.06	3	1.5	-7	3	360
4	2	0.06	3	1.5	-7	3	320

(Image1_ini)

| **(Image1)** | **(Image2)** | **(Image3)** | **(Image4)** |

Figure 10. Segmentation result of the third MRI images series. (Image1_ini) Initial curve in red color, (Image1), (Image2), (Image3), and (Image4) final curves

Table 5. Segmentation process parameters of the third MRI images series

Image No.	Sigma(σ)	Mu(μ)	Lambda(λ)	Epsilon(ε)	Alf(υ)	Delt(T)	IterNo.
1	1.5	0.06	3	1.5	-6	3	550
2	1.5	0.1	3	1.5	-6	2	450
3	2	0.1	3	1.5	-5	2	400
4	1.5	0.1	3	1.5	-6	2	470

4. Discussion

The developed model enables the segmentation of MRI image series by always keeping the curve inside the tumor region. The reasons for the success of the proposed development are:

1- Stability of the tumor position: The series of MRI images is actually organized or stored as a stack. The shape of the tumor changes across the series (the size of the tumor increases or decreases) but the position does not change almost as shown in Fig(8), Fig(9), and Fig(10). As if we have concentric tumor images. In other words, there is no significant motion as in video frames (for example, horizontal motion).

2- Determine the tumor shape complexity and the Evolution Percentage: Determining the Evolution Percentage depends on the complexity of the tumor shape where the correct determination of the tumor shape complexity leads to the correct determination of the Evolution Percentage. The Evolution Percentage has a key role in the success of the proposed development because it defines the area of the initial curves for all next MRI images of the series. The Evolution Percentage can be determined by giving the appropriate value for the (EP) parameter. Concerning the experiments of this research, the optimal value of (EP) was 25% for MRI images series that include a tumor of a regular shape. As for the MRI images series that include a tumor of an irregular shape, the optimal value of (EP) was 13%.

The moderate evolution of the curve: The moderate evolution causes the initial curves to remain inside the tumor regions in all MRI images of the series. The speed of evolution can be controlled by giving fair values for Delt(T) and Alf(υ) parameters. Concerning **the** experiments of this research, the optimal values of Delt(T) were (2 to 3) and the optimal values of Alf(υ) were (-3 to -8) as shown in Table(3), Table(4), and Table(5). Values of Alf(υ) are always negative to indicate that the curve is always inside the tumor region.

5.   Conclusion

This research presented a developed segmentation model in an important research area which is the medical image processing. The developed model overcame its limitation by two things:

1- Adding a new parameter (EP) by which the area of the initial curves (initial curves of the next MRI images) is determined
2- Moderate curve evolution achieved by giving a fair values for Delt(T) and Alf(v) parameters.

The developed model successfully segmented the MRI images series. The optimal values have been determined for the parameters on which the success of the developed model depended. The optimal value of (EP) were 25% for MRI images series that include a tumor of a regular shape and (13%) for the MRI images series that include a tumor of an irregular shape. The optimal values of Delt(T) were (2 to 3) and the optimal values of Alf(v) were (-3 to -8). These optimal values can be used directly by any operator in segmenting the MRI images series and obtaining good results.

References

[1] N. Sharma, L. Aggarwal, "Automated Medical Image Segmentation Techniques", Journal of Medical Physics, Vol. 35, No. 1, pp. 3-14, 2009.
[2] R. Koprowski, Medical and Biological Image Analysis, open access Vol., IntechOpen, 2018.
[3] P. Aggarwal, R. Vig, S. Bhadoria, and C. Dethe, "Role of Segmentation in Medical Imaging: A Comparative Study", *International Journal of Computer Applications*, Vol. 29, No. 1, pp. 0975-8887, 2011.
[4] M. Hesamian, W. Jia, X. He, and P. Kennedy, "Deep Learning Techniques for Medical Image Segmentation: Achievements and Challenges", *Journal of Digital Imaging,* Vol. 32, pp. 582–596, 2019.
[5] S. Pereira, A. Oliveira, V. Alves, and C. Silva, "On hierarchical brain tumor segmentation in MRI using fully convolutional neural networks: A preliminary study", In: *Proc. of International Conf. on Bioengineering,* Coimbra, Portugal, 2017.
[6] C. Xu, A. Yezzi, and J. prince, "On the Relationship between Parametric and Geometric Active Contours", In: *Proc. of International Conf. on Signals, Systems, and Computers,* California, USA, 2000.
[7] R. Hemalatha, T. Thamizhvani, A. Dhivya, J. Joseph, B. Babu and R. Chandrasekaran, *Active Contour Based Segmentation Techniques for Medical Image Analysis*, open access Vol., IntechOpen, 2018.
[8] Y. Rathi, N. Vaswani, A. Tannenbaum, and A. Yezzi, "Particle Filtering for Geometric Active Contours with Application to Tracking Moving and Deforming Objects", In: *proc. of IEEE Computer Society Conference on Computer Vision and Pattern Recognition*, 2005.
[9] Y. Rathi, N. Vaswani, A. Tannenbaum, and A. Yezzi, "Tracking Deforming Objects Using Particle Filtering for Geometric Active Contours", *IEEE Transaction on Pattern Analysis and Machine Intelligence,* Vol. 29, No. 8, pp. 1470-1475, 2007.
[10] V. Caselles, R. Kimmel, and G. Sapiro, "Geodesic Active Contours", *International Journal of Computer Vision*, pp. 61-79, 1997.
[11] K. Djemal, W. Puech, and B. Rossetto, "Geometric Active Contour Model Using Level Set Methods for Objects Tracking in Images Sequence", In: *Proc. of International Conf. on Sciences of Electronic, Technologies of Information, and Telecommunications,* Tunisia, 2004.
[12] S. Osher, J. Sethian, "Fronts propagating with curvature dependent speed: algorithms based on Hamilton-Jacobi formulations", *Journal of Computer and Physics*, vol. 79, pp. 12-49, 1988.
[13] X. Bresson, "Image Segmentation with Variational Active Contour", Thesis, Faculty of Engineering Sciences and Techniques (STI), Switzerland, 2005.

[14] X. Jiang, R. Zhang, and S. Nie, "Image Segmentation Based on Level Set Method", In: *Proc. of International Conf. on Medical Physics and Biomedical Engineering*, 2012.

[15] C. Li, C. Xu, C. Gui, and M. Fox, "Level Set Evolution without Re-initialization: A New Variational Formulation", In: *proc. of the IEEE Computer Society Conference on Computer Vision and Pattern Recognition*, 2005.